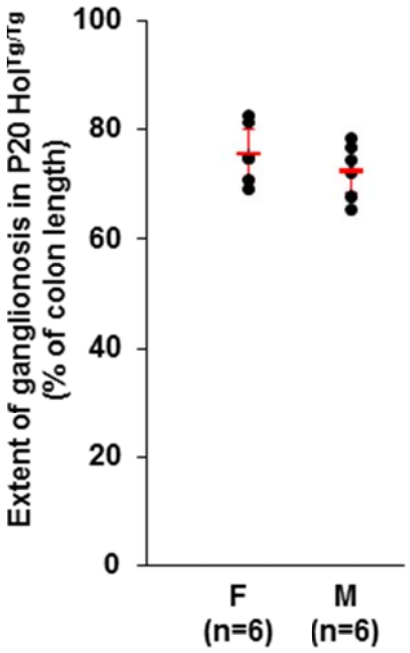

Figure S1. Extent of aganglionosis is similar in male and female Hol$^{Tg/Tg}$ animals. Quantification of the length of the ganglionated zone (in % of total colon length) in the colon of P20 Hol$^{Tg/Tg}$ animals via staining of acetylcholinesterase activity. Data are presented as the mean ± SEM. No significant difference was observed according to a Student's *t*-test.

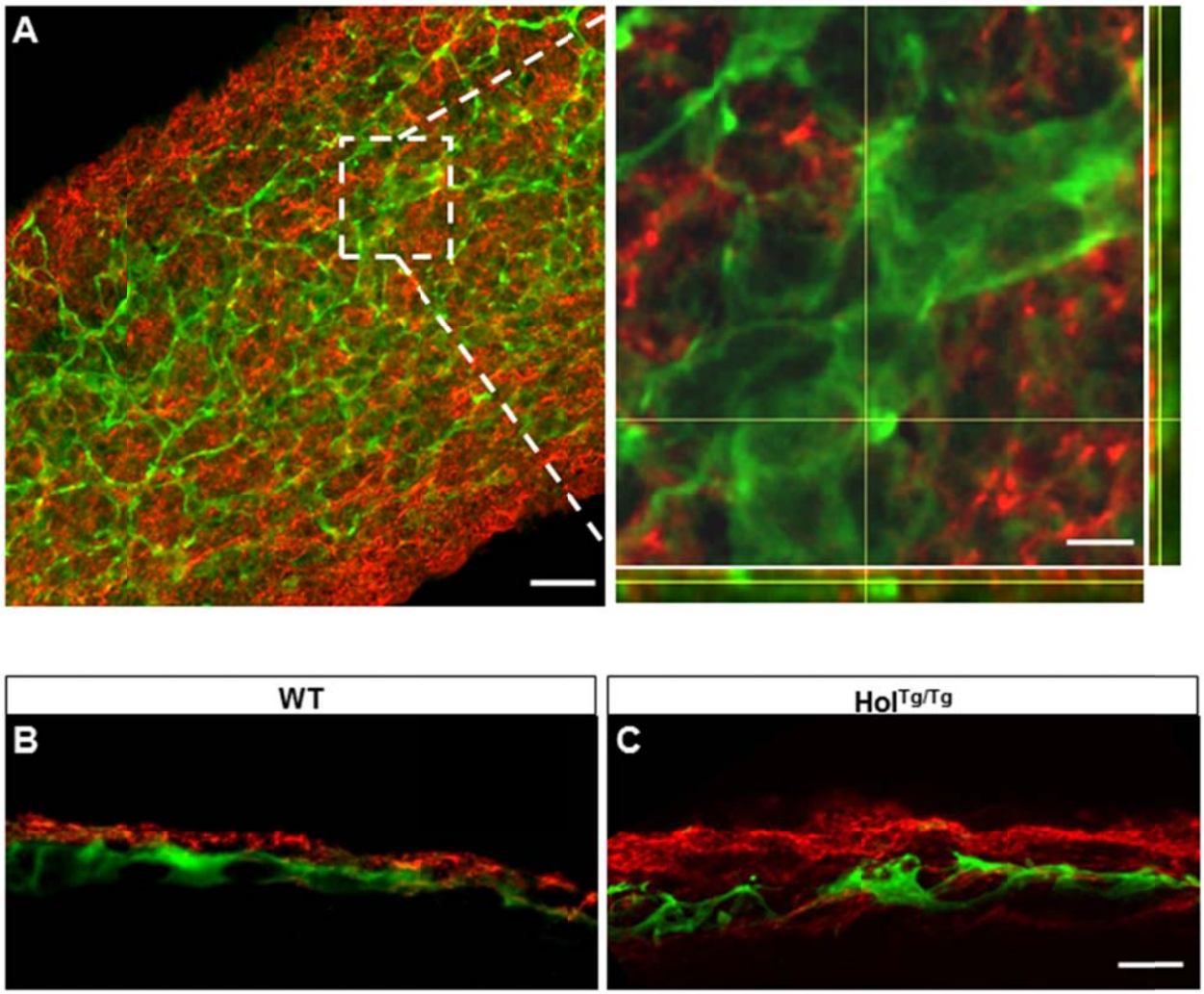

Figure S2. Collagen VI is juxtaposed to eNCC in $Hol^{Tg/Tg}$ **embryonic intestines.**
(A-C) Double immunofluorescence labelling of e15.5 small intestines performed with antibodies against βIII-Tubulin (green) and collagen VI (red). **(A)** Z-stack projection of a whole-mount preparation showing that high levels of collagen VI are present in a mutually exclusive manner around neuronal-fated eNCC in a $Hol^{Tg/Tg}$ embryo. **(A')** Zoom-in view of the region delimited by the white square in A. Lateral views of the *z*-axis along the *x* and *y* axes (at the level indicated by white lines) are shown on the right and lower panels, respectively. **(B-C)** Single confocal sections of transverse vibratome slices comparing WT (B) and $Hol^{Tg/Tg}$ (C) tissues. Scale bar, 20µm (5µm in A').

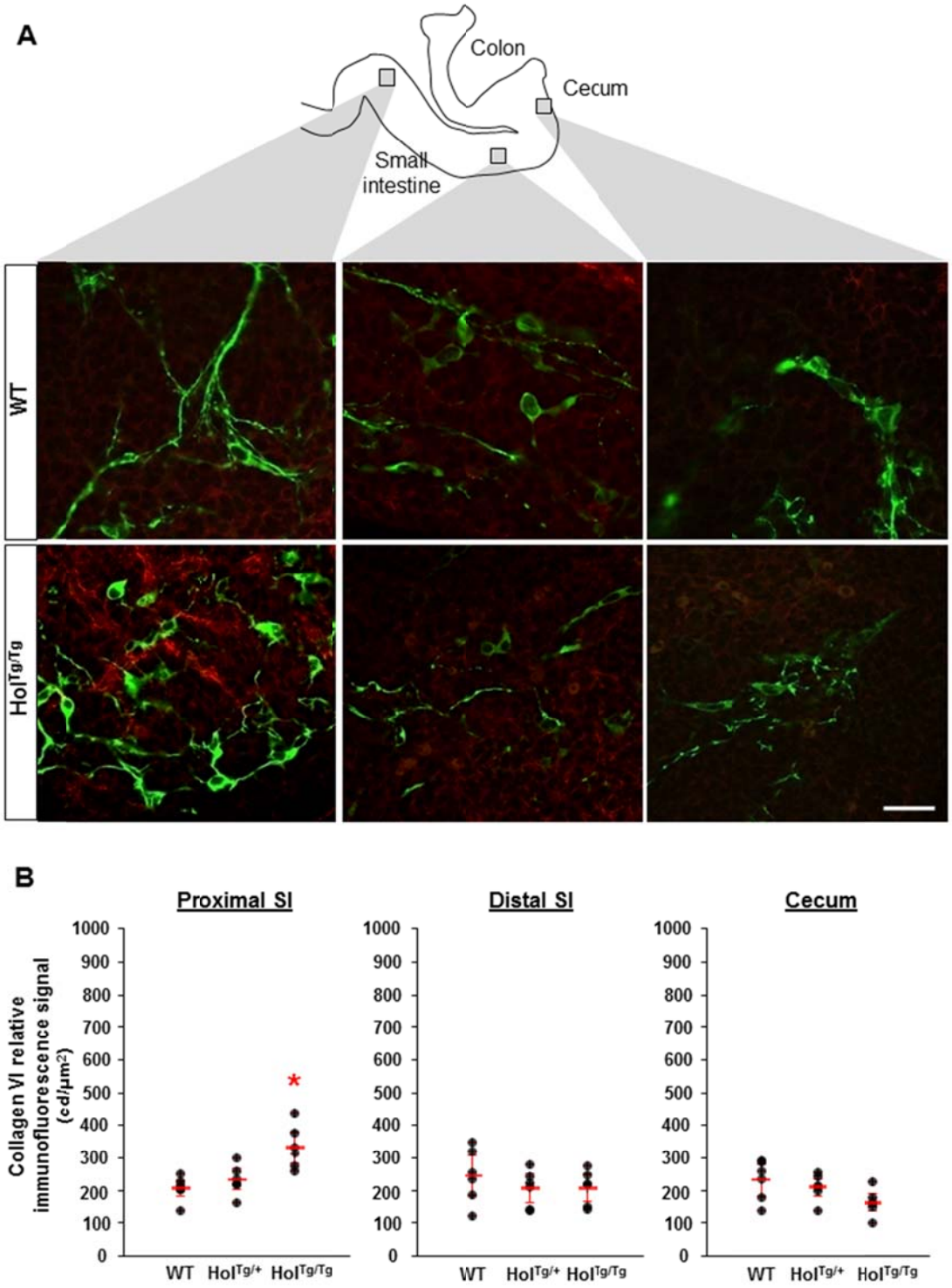

Figure S3. Collagen VI protein levels are increased in e11.5 Hol$^{Tg/Tg}$ intestines.
(A) Single confocal sections in the plane of the developing myenteric plexus in wild-type (upper panels) and Hol$^{Tg/Tg}$ (lower panels) e11.5 intestines doubly labelled with anti-collagen VI (red) and anti-βIII-Tubulin (green) antibodies. Scale bar, 20µm. **(B)** Quantification of collagen VI immunofluorescence signals in candelas (cd) per µm^2 showing that collagen VI protein levels are significantly increased only in regions of Hol$^{Tg/Tg}$ embryonic intestines that contain a high number of neuronal-fated eNCC (data are presented as the mean ± SEM; n=6 intestines per genotype; *$p < 0.05$; one-way ANOVA). SI, small intestine.

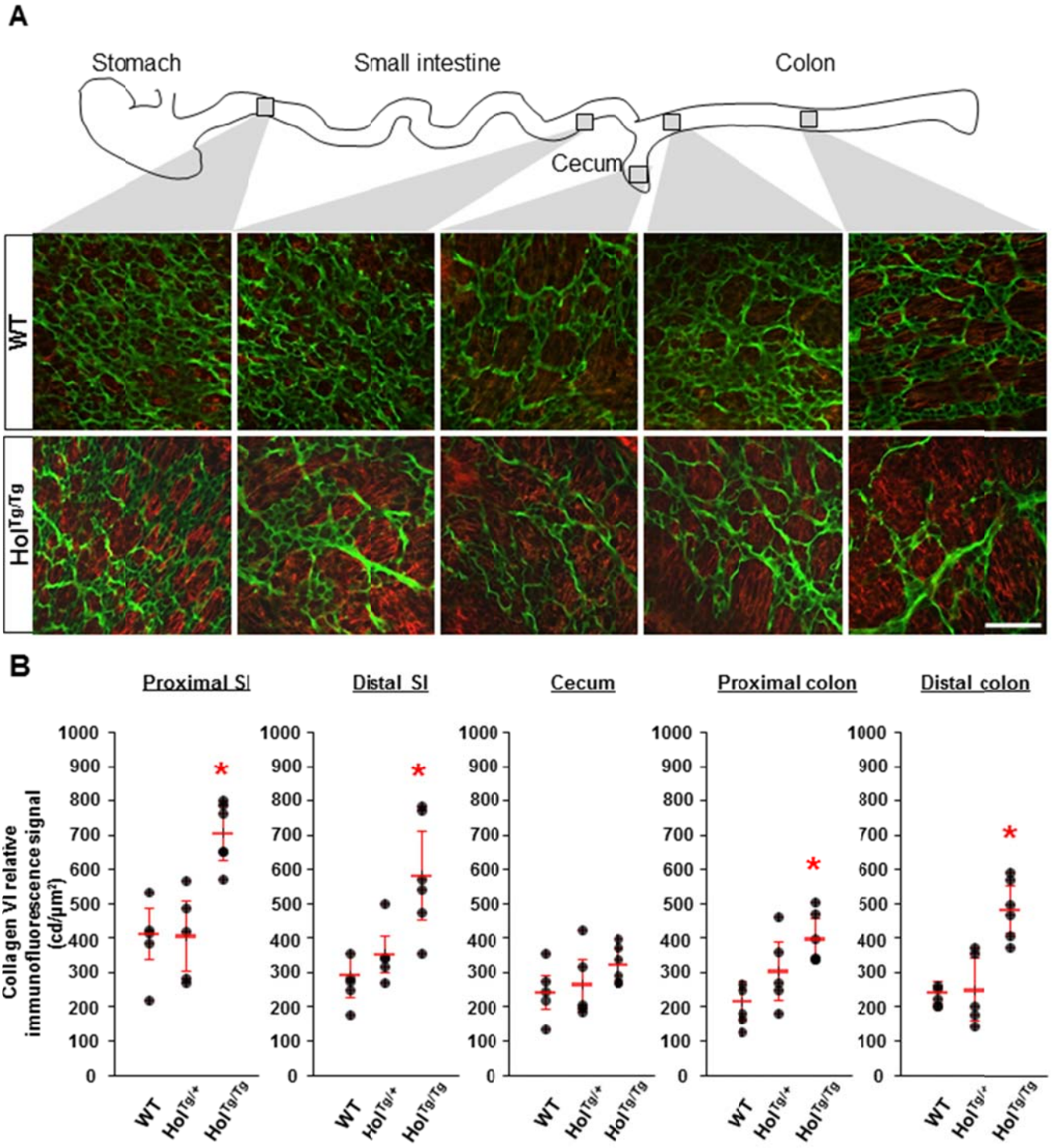

Figure S4. Collagen VI protein levels are increased in e15.5 Hol$^{Tg/Tg}$ intestines.
(A) Single confocal sections in the plane of the developing myenteric plexus in wild-type (upper panels) and Hol$^{Tg/Tg}$ (lower panels) e15.5 intestines doubly labelled with anti-collagen VI (red) and anti-βIII-Tubulin (green) antibodies. Scale bar, 20µm. **(B)** Quantification of collagen VI immunofluorescence signals in candelas (cd) per µm^2 showing that, in comparison to WT, collagen VI protein levels are significantly increased in the entire Hol$^{Tg/Tg}$ embryonic intestines except the cecum (data are presented as the mean ± SEM; n=6 intestines per genotype; *$p < 0.05$; one-way ANOVA). SI, small intestine.

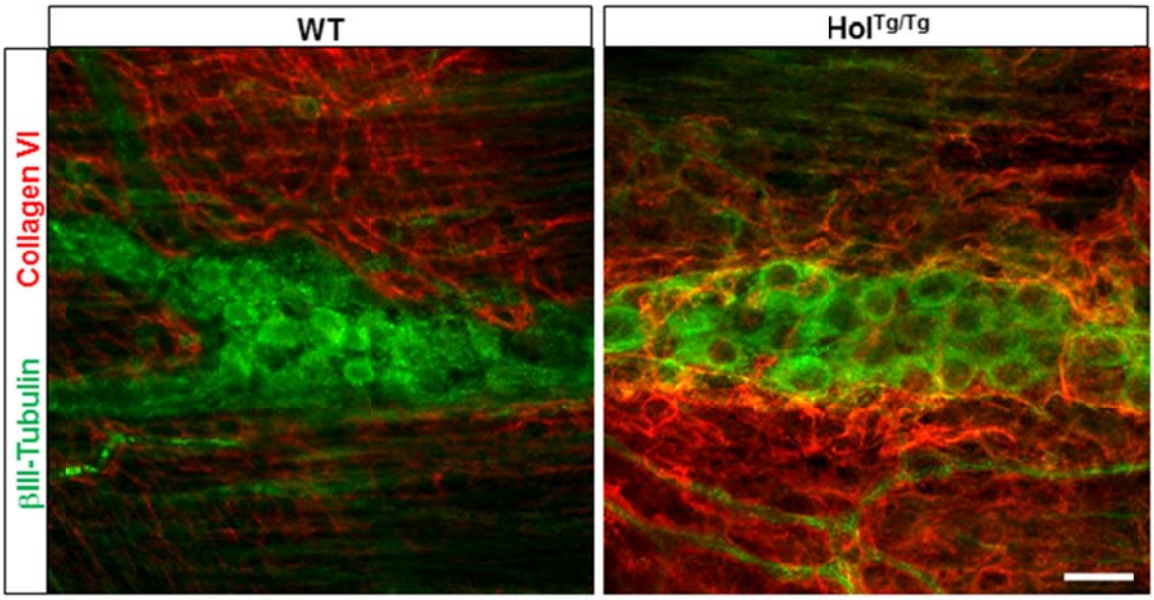

Figure S5. High levels of collagen VI are aberrantly present around and within myenteric ganglia of post-natal Hol$^{Tg/Tg}$ animals.

Single confocal sections of 3-week old colons double labelled with antibodies against βIII-Tubulin (green) and collagen VI (red). In contrast to wild-type tissues, abundant collagen VI is found both around and within myenteric ganglia from Hol$^{Tg/Tg}$ mice. Scale bar, 20μm.

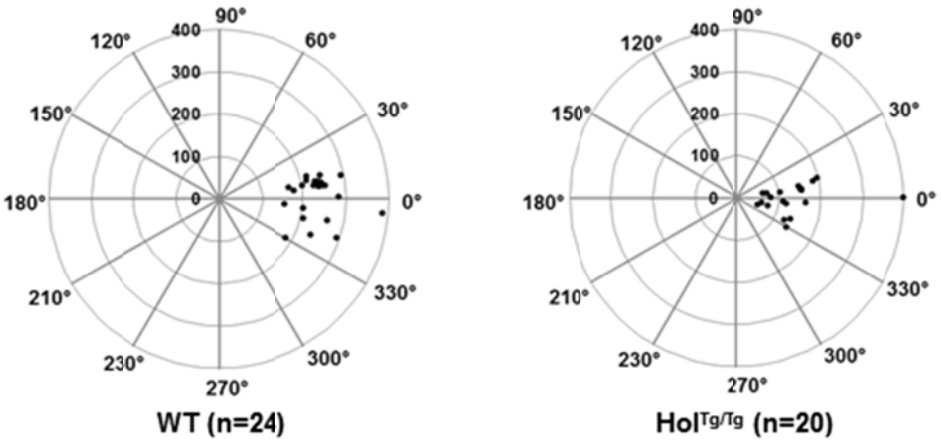

Figure S6. Cell migration directionality is unaffected in Hol$^{Tg/Tg}$ eNCC.
Polar histograms showing the net trajectories (in degrees) and traveled distance (in μm) of individual eNCC at the migration front in e12.5 embryos. No difference in directionality was detected between WT and Hol$^{Tg/Tg}$ eNCC (Student's *t*-test).

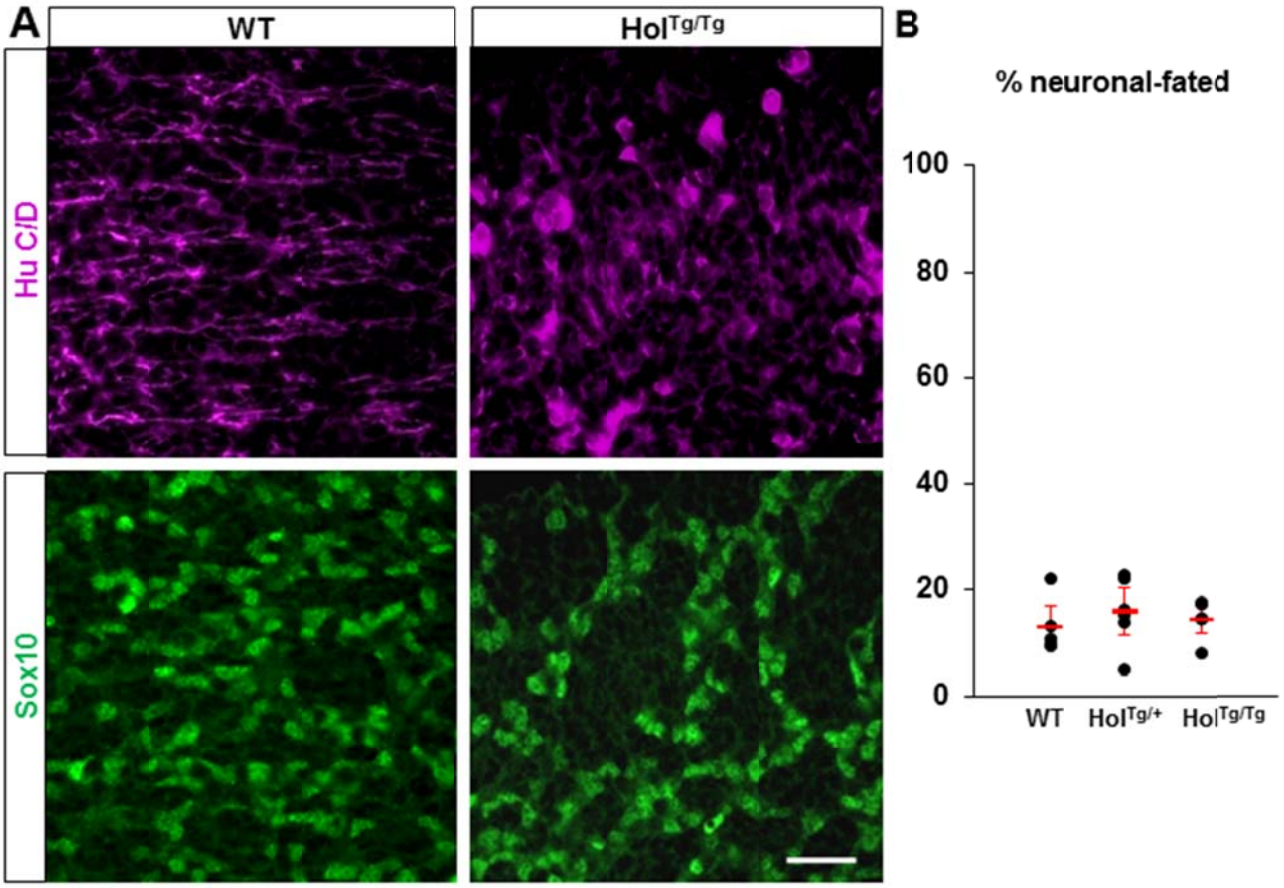

Figure S7. Neuronal differentiation of Hol$^{Tg/Tg}$ eNCC at e12.5.
(A) Single confocal sections of e12.5 small intestines double labelled with antibodies to allow identification and discrimination of neuronal-fated (Sox10^{-} HuC/D^{+}) and undifferentiated (Sox10^{+} HuC/D^{-}) eNCC. Scale bar, 20µm. **(B)** Quantitative analysis of the relative abundance of neuronal-fated eNCC (in %) within the whole eNCC population which is represented by the combined number of Sox10^{+} cells and HuC/D^{+} cells (data are presented as the mean ± SEM; n=5 intestines per genotype). No statistically significant differences between group means were noted according to one-way ANOVA.

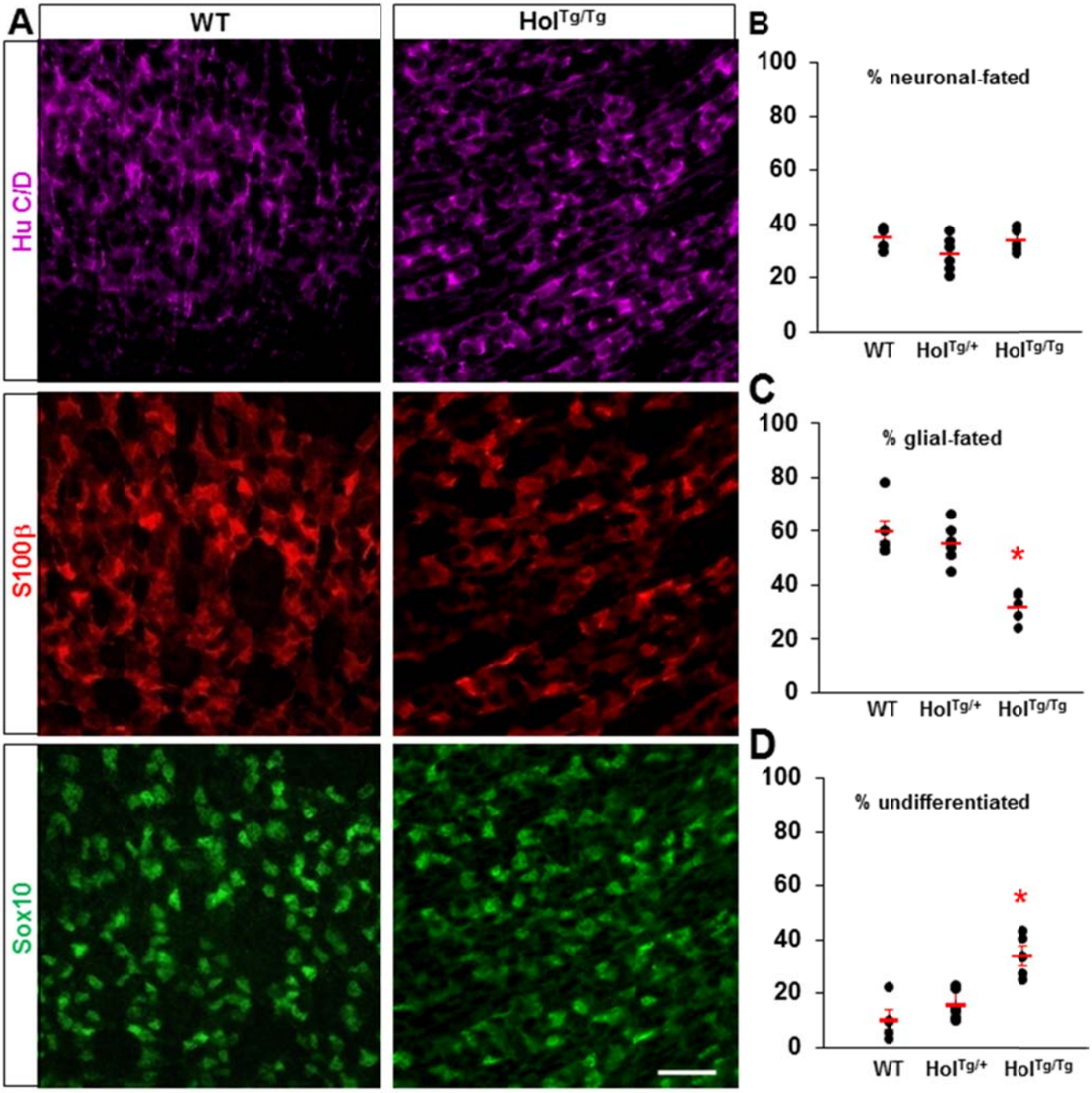

Figure S8. Neuronal and glial differentiation of Hol$^{Tg/Tg}$ eNCC at e15.5.
(A) Single confocal sections of small intestines triple labelled with antibodies to allow identification and discrimination of neuronal-fated (Sox10$^-$ HuC/D$^+$ S100β$^-$), glial-fated (Sox10$^+$ HuC/D$^-$ S100β$^+$) and undifferentiated (Sox10$^+$ HuC/D$^-$ S100β$^-$) eNCC. Scale bar, 20µm. **(B-D)** Quantitative analysis of the relative abundance of each subset (in %) within the whole eNCC population which is represented by the combined number of Sox10$^+$ cells and HuC/D$^+$ cells (data are presented as the mean ± SEM; n=6 intestines per genotype; *$p < 0.05$; one-way ANOVA). A decreased number of glial-fated eNCC to the benefit of undifferentiated progenitors is noted in Hol$^{Tg/Tg}$ tissues.

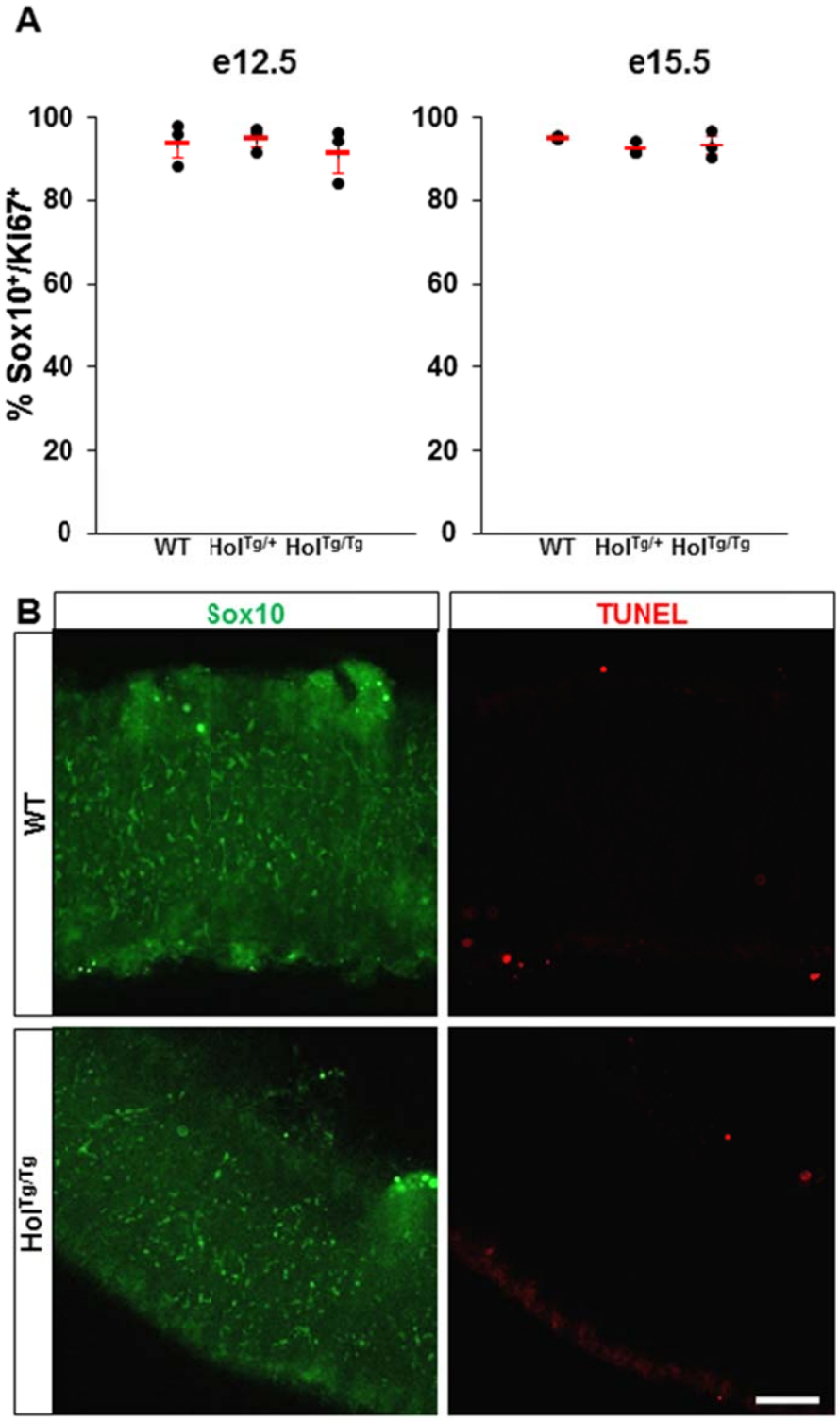

Figure S9. Proliferation and survival of Hol$^{Tg/Tg}$ eNCC.
Cell proliferation (**A**, at e12.5 and e15.5) and cell death (**B**, at e12.5) were evaluated in the small intestines of wild-type and Hol$^{Tg/Tg}$ embryos using nucleic markers for proliferation (Ki67) and for DNA fragmentation (TUNEL), respectively. Counts were restricted to Sox10^{+} cells. No significant variation was observed according to one-way ANOVA (data are presented as the mean ± SEM; n=3 intestines per genotype). Scale bar, 50µm.

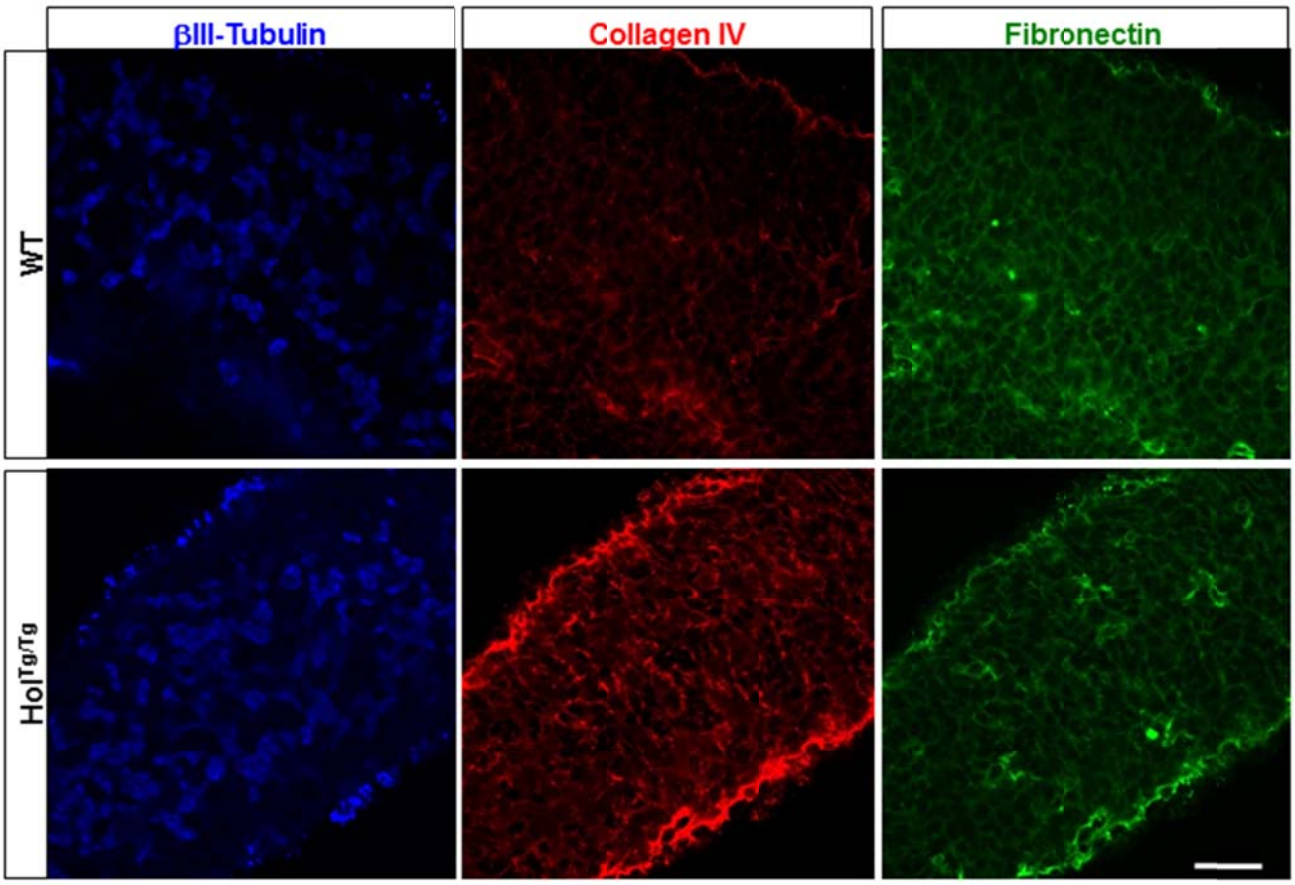

Figure S10. Fibronectin remains unaffected in Hol$^{Tg/Tg}$ embryonic intestines.
Single confocal sections of e15.5 small intestines triple labelled with antibodies against βIII-Tubulin (blue), collagen VI (red) and fibronectin (green), showing that higher collagen VI levels in Hol$^{Tg/Tg}$ bowels have no overt impact on fibronectin levels and organization.

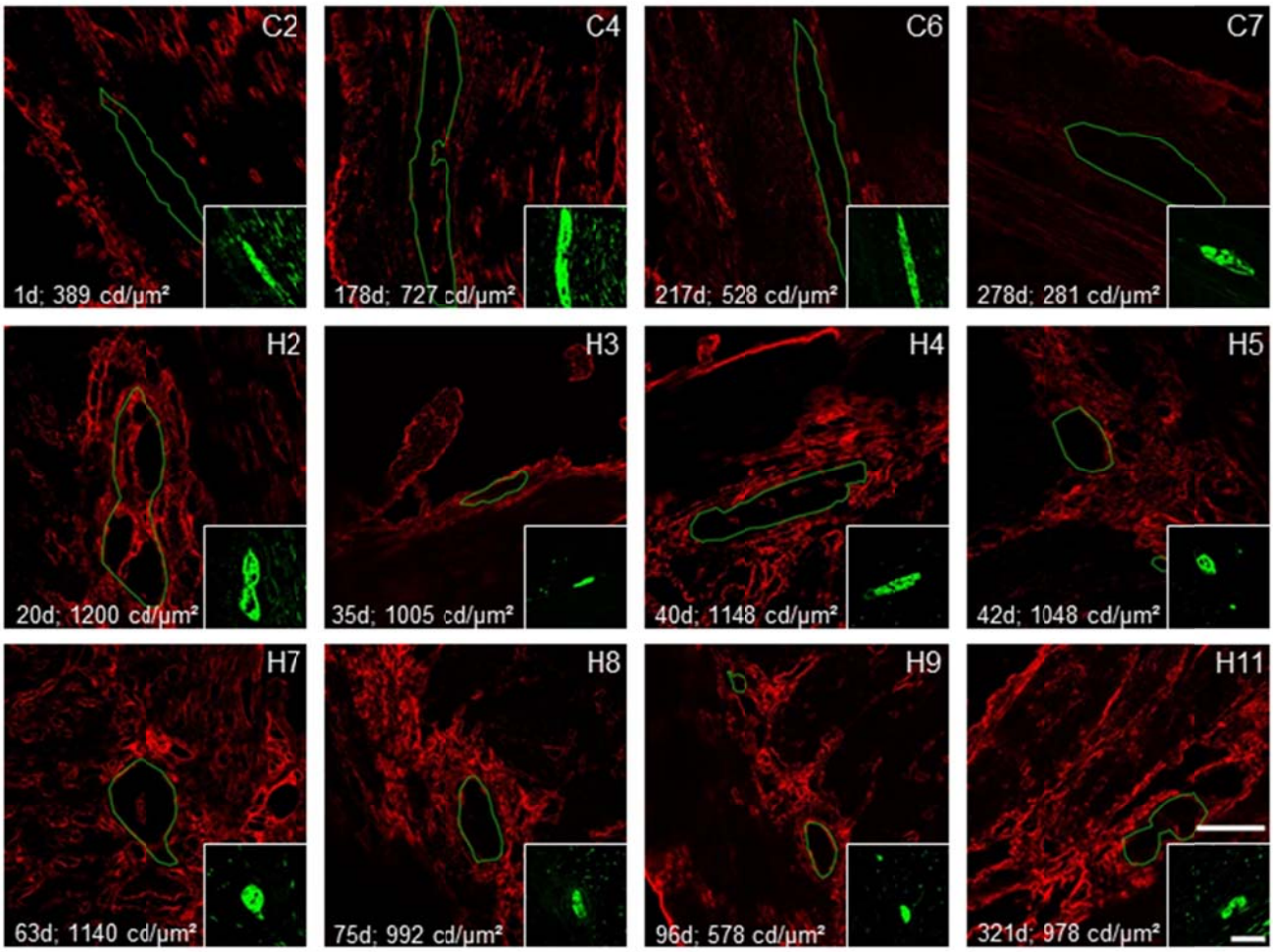

Figure S11. Tested human colonic tissues not included in Figure 7.
Representative single confocal sections of transverse cuts of human colonic muscles double-labeled with antibodies against βIII-Tubulin (green; in the insets) and collagen VI (red). Myenteric ganglia are delineated by green lines. Identification number of controls (C), HSCR patients (H) and Down-HSCR patients (D) is indicated in the upper right corner. Age at the time of tissue collection (indicated in days (d)) as well as average level of peri-ganglionic collagen VI (n≥5 ganglia/child's sample; expressed in candelas (cd) per μm^2) are indicated in the lower left corner. Scale bar, 50µm (75µm in insets).

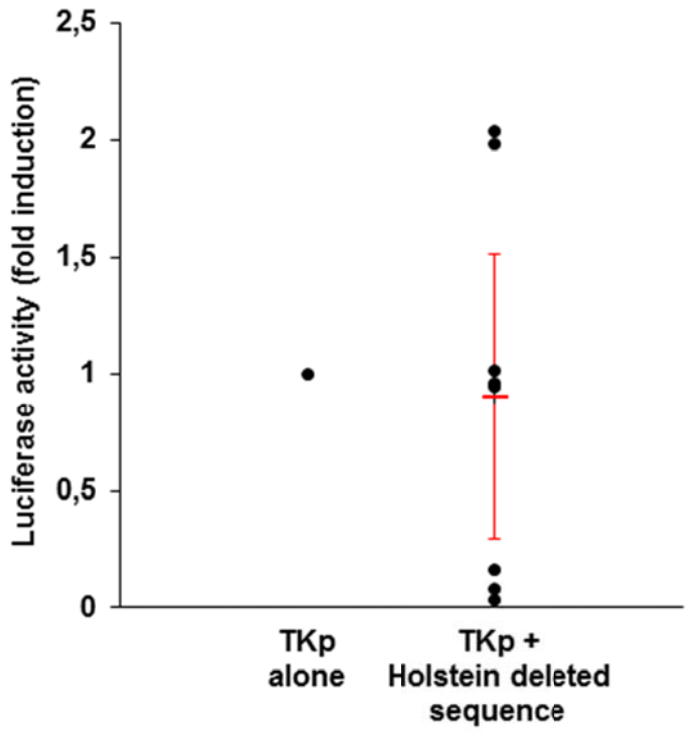

Figure S12. The 153bp deletion at the Holstein locus is devoid of consistent regulatory activity. Evaluation of transcriptional activity for the small block of sequences deleted by the transgenic insertion in the Holstein genome. Luciferase assays were performed in Neuro2a cells with reporter constructs driven by the minimal TK promoter +/- the 153bp fragment of deleted sequences. Luciferase activity is reported in fold induction relative to the vector only driven by the TK minimal promoter (data are presented as the mean ± SEM; n=9 independent experiments performed in triplicate). No significant difference was noted according to a Student's *t*-test.

Table S1. Patients' characteristics and full collagen VI quantification data for all tested human samples.

ID	Age (in days)	Gender (M or F)	Mean peri-ganglionic collagen VI levels (in candelas/μm^2)	Mean intra-ganglionic collagen VI levels (in candelas/μm^2)
C1	1	M	780	390
C2	1	M	389	346
C3	60	M	401	195
C4	178	M	727	409
C5	191	M	123	211
C6	217	F	528	278
C7	278	M	281	149
C8	452	M	321	211
H1	17	M	1200	374
H2	20	M	1200	646
H3	35	F	1005	622
H4	40	M	1148	413
H5	42	M	1048	419
H6	51	M	773	194
H7	63	M	1140	514
H8	75	F	992	436
H9	96	M	578	293
H10	222	M	969	421
H11	321	M	978	363
H12	454	M	633	341
D1	49	F	1358	389
D2	97	M	1201	647
D3	182	M	1049	537
D4	336	M	1659	640

Note: *Age is at time of tissue collection.*

Table S2. Details of the oligonucleotide primers used for RT-PCR and genotyping

ID	Sense primer	Antisense primer
Wdr82	5'-CAGTATGATAGGACCTGTGAGTGG	5'-AGCCACTTTTATACCACTCTCTCC
Glyctk	5'-CTATCCTGCTCAGGTGATAAGCC	5'-TTGAGAATATGCAGGCAGTCTTGC
Col6a4	5'-AAGAGGATTTTCAGGAGAGAAGGG	5'-AGATTATCAATTCCAGGATCCCCC
Col6a5	5'-GTGACTCAGTACAGGGAAGGG	5'-GTGGTCCCCCACTGACTCATC
Col6a6	5'-TCAGCATCTGGCCTGTTAGG	5'-CGTACTCGGGGCCAGAATCTT
Genotyping F	5'-GTGGTGGACCTAACCTTACAAGGA	n/a
Genotyping R1	n/a	5'-CAGGGCTAAGTCTTGGCTTACTTG
Genotyping R2	n/a	5'-CACAGCTTGCTGTATCAGAGCCAT

Table S3. Characteristics of the primary and secondary antibodies used in this study

Antibody	Host species	RRID number	Source
Anti-βIII-Tubulin	Mouse	AB_2256751	Abcam, ab78078
Anti-collagen VI	Rabbit	AB_305585	Abcam, ab6588
Anti-Sox10	Goat	AB_2195374	Santa Cruz Biotechnology, sc-17342
Anti-S100β	Rabbit	AB_10013383	DakoCytomation, Z0311
Anti-HuC/D	Mouse	AB_2314656	Molecular Probes, A-21271
Anti-Ki67	Rabbit	AB_443209	Abcam, ab15580
Anti-Goat Alexa Fluor 488	Bovine	AB_2340883	Jackson ImmunoResearch, 805-545-180
Anti-Rabbit Alexa Fluor 594	Donkey	AB_2340621	Jackson ImmunoResearch, 711-585-152
Anti-Mouse Alexa Fluor 647	Donkey	AB_2340862	Jackson ImmunoResearch, 715-605-150

Supporting information

Supplemental Acknowledgments: The following French Departments of Pediatric Surgery from the Ente-Hirsch study group are thanked for participating to this work: Etienne Suply, Stephan de Napoli, Marc-David Leclair (University Hospital of Nantes); Guillaume Levard, Véronique Couvrat-Carcauzon (University Hospital of Poitiers); Philine de Vries (University Hospital of Brest); Guillaume Podevin (University Hospital of Angers); Sabine Sarnacki, Erik Hervieux (Necker Hospital, Hospital for Sick Children, Paris).

Movie S1: Example of eNCC migration in an e13.5 control embryo.

Movie S2: Example of eNCC migration in an e13.5 Hol$^{Tg/Tg}$ embryo.

Supplemental Dataset 1: Full rRNA-depleted transcriptome of e12.5 WT::G4-RFP and Hol$^{Tg/Tg}$::G4-RFP eNCC